Received April 2, 2019, accepted April 17, 2019, date of publication April 29, 2019, date of current version May 10, 2019.

Digital Object Identifier 10.1109/ACCESS.2019.2913726

Shared Aperture Metasurface for Bi-Functions: Radiation and Low Backward Scattering Performance

CHEN ZHANG, XIANGYU CAO, (Senior Member, IEEE), JUN GAO, SI-JIA LI, HUANHUAN YANG, (Student Member, IEEE), TONG LI, AND DI ZHANG
Information and Navigation College, Air Force Engineering University, Xi'an 710077, China

Corresponding author: Chen Zhang (xue320long@sina.cn)

This work was supported in part by the NSFC under Grant 61671464, Grant 61701523, and Grant 61801508, in part by the Postdoctoral Innovative Talents Support Program of China under Grant BX20180375, in part by the Natural Science Foundational Research Fund of Shaanxi Province under Grant 2017JM6025 and Grant 2018JM6040, and in part by the Young Talent fund of University Association for Science and Technology in Shaanxi, China, under Grant 20170107.

ABSTRACT In this paper, a novel method to design a multifunctional metasurface (MS) is proposed and demonstrated. Inspired by shared aperture technology, the proposed MS is integrated with both radiation and low backward scattering performance. Each MS unit cell consists of two parts, polarization conversion surface part and radiation part. Different from traditional MS design, the proposed two parts are integrated together, and thus, bi-functions are realized in one surface. To acquire radiation performance, the feeding structure is added to each radiation in part by introducing an antenna design concept. The peak gain of the MS attains 18.1 dBi and main-beam patterns are all along the normal direction. To obtain low backward scattering performance, the polarization of an incident electromagnetic wave is transformed by the reflected MS. The reflected wave will have a 180° phase difference through rotating the polarization conversion surface structure. Thus, two different types of MS units are arranged in chessboard array to achieve reflection suppression. The radar cross section reduction band is from 3.0 to 4.3 GHz with peak values of 7.2 and 16.8 dB. Both the simulated and experimental results prove that our method offers a feasible strategy for the multifunctional MS design which can lead to many exciting applications in different frequency domains.

INDEX TERMS Metasurface, shared aperture technology, radiation, low backward scattering.

I. INTRODUCTION

Metasurfaces (MSs) are normally defined as two-dimensional surface constructed by inhomogeneous arrangements of subwavelength metallic or dielectric inclusions [1]–[3]. Till now, plenty of fascinating optical and electromagnetic (EM) phenomena have been generated using MS such as anomalous refraction/reflection [4]–[6], polarization rotation [7]–[9], orbital angular momentum (OAM) vortex waves [10]–[12], and surface wave conversion [13]–[17]. These features can be achieved through flexible designs and elaborate arrangements of MS elements. With the merits of low profile, low cost and conformal ability, MSs have received intensive exploitation, particularly in stealth domain [18]–[21].

There are two main types of MSs which can achieve low scattering properties. The first one is absorbing MS which transforms the EM waves into heat energy and reduces the reflection of target. This type of MS was firstly proposed by Landy in 2008 and named as perfect metamaterial absorber (PMA) [22]. Later, various efforts on PMA have been made to achieve wide incidence, polarization-insensitive, tunable, and wideband absorption [23], [24]. The second one is reflective MS which can redirect the incident waves to non-threatening space [25], [26]. A representative MS design for this type is the combination of artificial magnetic conductor (AMC) and perfect electric conductor (PEC) in a chessboard configuration [27]. Based on this method, a series of improved reflective MSs have been designed [28], [29]. For instances, adopting two or three different AMC elements can broaden the low scattering bandwidth, besides, polarization conversion surfaces (PCSs) are also used to construct the MS [30], [31]. Recently, the research on MS has developed rapidly. Numerous novel MSs have aroused researchers' widespread concern, such as

The associate editor coordinating the review of this manuscript and approving it for publication was Kuang Zhang.

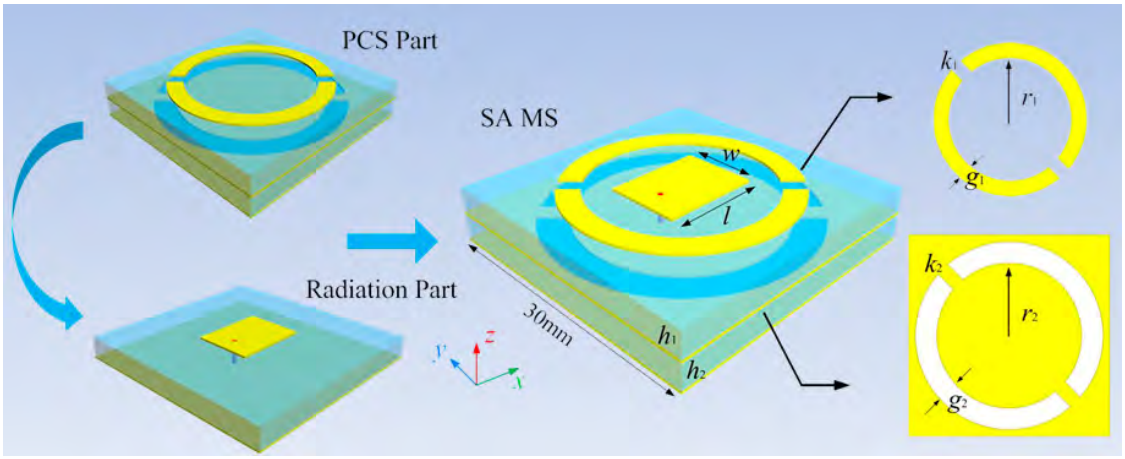

FIGURE 1. Schematic geometry of the proposed MS unit cell. Design parameters of the elements are w = 8mm, l = 10.5mm, h1 = 3mm, h2 = 3mm, r1 = 9.6mm, r2 = 10.8mm, g1 = 2.4mm, g2 = 3.2mm, k1 = 2mm, k2 = 2.2mm.

coding and multifunctional MS. Through adopting optimization algorithms and other special design method, both low scattering property, and other multiple functions are obtained [32]. In summary, these pioneering MSs possess powerful abilities to achieve low scattering performance.

As one promising application, low scattering MSs could be utilized in stealth domain, especially reducing the reflection of antennas. Ref. [33] loaded three-layer PMA around guidewave solt array antennas, the in-band reflection is reduced and antenna radiation property is maintained. Ref [34] designed a low scattering partially reflected surface (PRS)-antenna, the antenna can achieve low scattering and high gain properties at the same time. Besides, numerous similar references all realized antenna low scattering properties using different types of MSs [35]–[37]. Although the above literatures have made great progress, the MS applications still have some defaults. For example, the MS radiation and scattering parts are not integrated. After loading MS, antenna aperture usually needs to be increased to ensure radiation properties and the design complexity raises. The shared aperture (SA) technology is originally used in the field of phased arrays. Different sized antenna patches are installed in the same aperture area thus a space-filled design is obtained [38]. The advantage of this concept is enabling the antennas to operate at different frequency bands and polarizations, so that a same sized physical area could obtain more properties. Similarly, it also has great potential to design MS with integrated radiation and low backward scattering properties using SA technology.

Inspired by SA technology, we propose a novel MS with integrated radiation and low backward scattering performances. Each MS unit cell consists of two structures, PCS part and radiation part. Different from traditional MS design, the proposed two parts are integrated in one surface to realize different functions. To acquire radiation performance, feeding structure is added to each radiation part by introducing antenna design concept. Concurrently, the incident EM wave polarization is transformed after irradiating each MS units. The reflected wave will have a 180° phase difference only through rotating the PCS structure. To acquire low backward scattering performance, these two different types of MS elements (rotating PCS part or not) are designed and arranged in a chessboard array. Both simulations and measurements prove the correctness of the proposed SA MS design, which can lead to many exciting applications in different frequency domains.

II. DESIGN AND ANALYSIS OF SHARED APERTURE METASURFACE UNIT CELL

The key step of the MS design is that a single unit cell should possess radiation property and the ability to manipulate incident waves simultaneously. Thus the SA concept is utilized, a PCS structure and a radiation structure are integrated together, sharing the same aperture and realize different functions. The schematic of the proposed SA MS unit cell is presented in Fig. 1. PCS part is a two-layer structure with patterns etched on the substrate. A spilt ring resonator (SRR) is on the top, a complementary structure is in the middle and a metallic ground is installed on the bottom. The substrate is FRA with dielectric constant of 2.65, the patterns are copper with the conductivity of 5.8×107 S/m and the thickness is 0.036mm. Radiation part is a single square metal patch with a feeding structure. The unit cell is fed with 50Ω coaxial probes for the purpose of impedance matching.

Numerical simulation is carried out to investigate the performance of the proposed MS unit cell by using Ansoft HFSS. First, the polarization conversion property is analyzed. Two Floquet ports are adopted and periodic boundary conditions set to its four lateral sides for modeling infinite array. The reflection coefficients for both x- and y-polarized waves are simulated, as shown in Fig. 2(a). r_{xx} and r_{yy} represent the same polarized coefficients. r_{yx} and r_{xy} represent conversion coefficients.

From 2.9GHz to 4.1GHz, r_{yx} and r_{xy} are higher than $-$ 2dB which indicates most incidences have been transformed. Fig. 2(b) shows polarization conversion rates (PCRs) of the

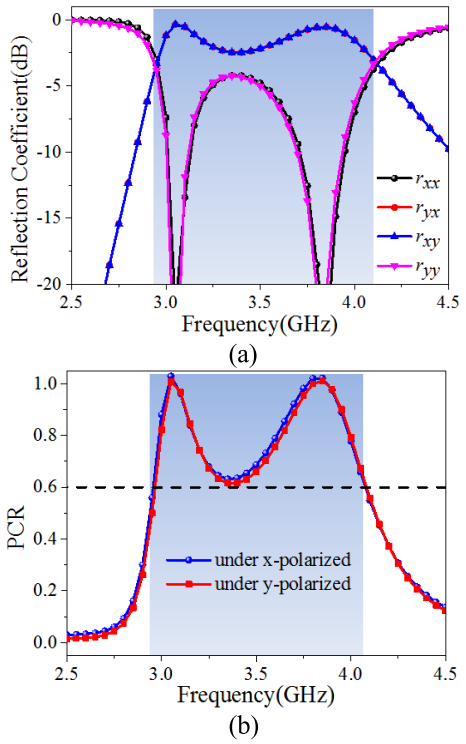

FIGURE 2. Polarization conversion properties of MS unit cell. (a) Reflection coefficient for x-polarized waves, (b) polarization conversion rate.

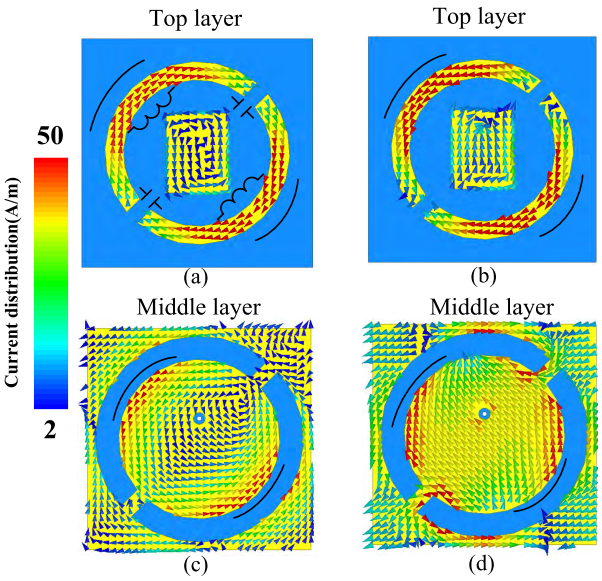

FIGURE 3. Current distributions of MS unit cell for x-polarized waves. (a) Top layer and (b) middle layer current distributions at 3.05GHz. (c) Top layer and (d) middle layer current distributions at 3.85GHz.

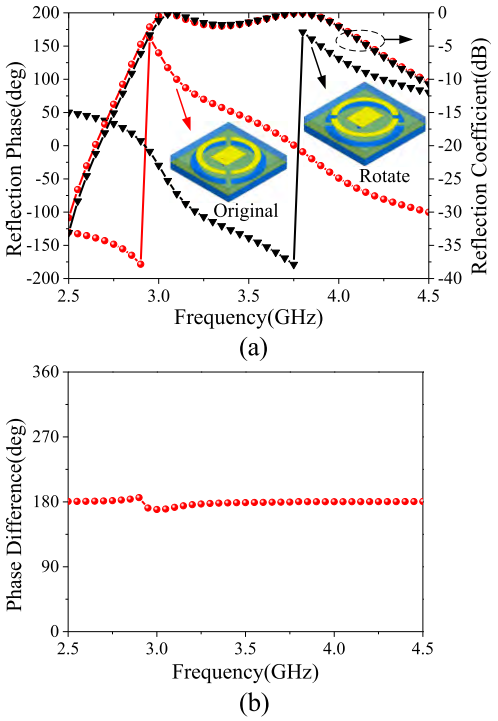

FIGURE 4. Reflection properties of MS unit cell before and after rotation. (a) Reflection phases and coefficients, (b) phase difference.

proposed unit cell. It can be seen the PCRs are higher than 0.6 from 2.95GHz to 4.05GHz. At 3.05GHz and 3.85GHz, there are two peak values closing to 1.0 which indicates almost all incident waves have been transformed. In addition, both the reflection coefficients and PCR curves are basically coincident under different polarized incidences. Since the PCS part is a symmetrical structure, the results show that radiation square patch has little impact on polarization conversion properties. To further verify the analysis, current distributions on the top and middle layers at two resonance frequency points are investigated. As Fig. 3(a) and 3(b) show, the current distributions on the SRR structures are stronger than those on the square patches. This phenomenon indicates that the SRR structures are the main factor to realize polarization conversion properties. At these two frequency points, different types of resonance occur. The current distribution on the top layer is in one direction at 3.05GHz. Two ring metal patches can be equivalent to inductances, and two gaps between the patches can be equivalent to capacitances. At 3.85GHz, the current direction is opposite. At present, two ring metal patches can be equivalent to two symmetrical dipoles. Consequently, we can conclude that a capacitance-inductance type resonance occurs at 3.05GHz and a dipole type resonance occurs at 3.85GHz. Owing to these two different resonance forms, such wideband polarization conversion properties can be achieved. As can be seen in Fig. 3(c) and 3(d), the current distributions on the middle layer are different from those on the top layer, which indicates that interaction is produced between them. Therefore, the correctness of the proposed MS design is further verified.

Through rotating PCR part of the proposed MS unit cell, an obvious phase difference will exist between the two structures, as shown in Fig. 4(a). For x-polarized incident wave, reflection coefficients of two curves are basically coincident. The reason is that the designed PCS part is a

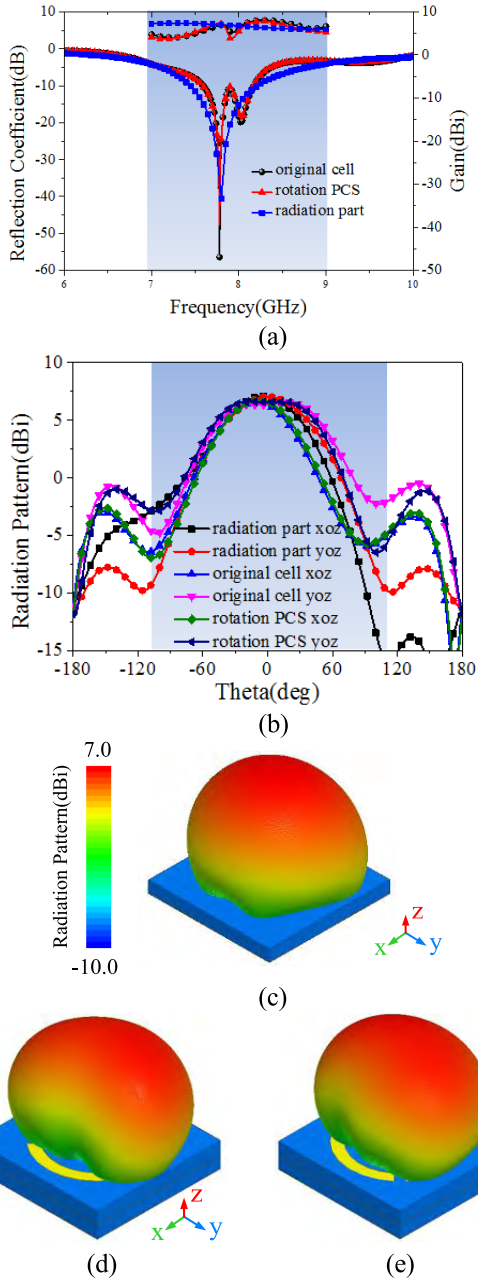

FIGURE 5. Radiation properties among three different unit cells. (a) Reflection coefficients. (b) 2D radiation patterns at resonant frequencies. (c), (d), (e) 3D radiation patterns at resonant frequencies.

symmetrical structure. Reflection phases of two structures have a difference nearly to 180°, shown in Fig. 4(b). The simulated results agree well with theoretical analysis [39]. Thus, the scattering properties of the whole MS array can be manipulated through arranging these two different units into different sequences [32].

Once the feeding structure is excited, the MS unit cell can be regarded as an antenna element with radiation performance. For the whole MS unit cell, the radiation part is the main factor while the PCS part affects smaller on radiation properties. In order to make a more detailed explanation on radiation properties, a comparison among original MS

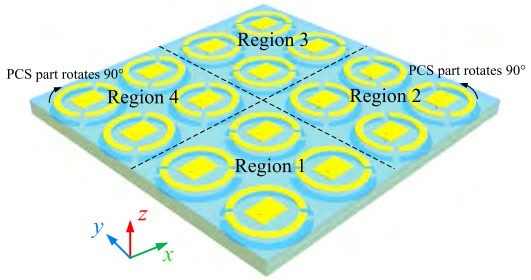

FIGURE 6. Schematic geometry of chessboard configuration MS array.

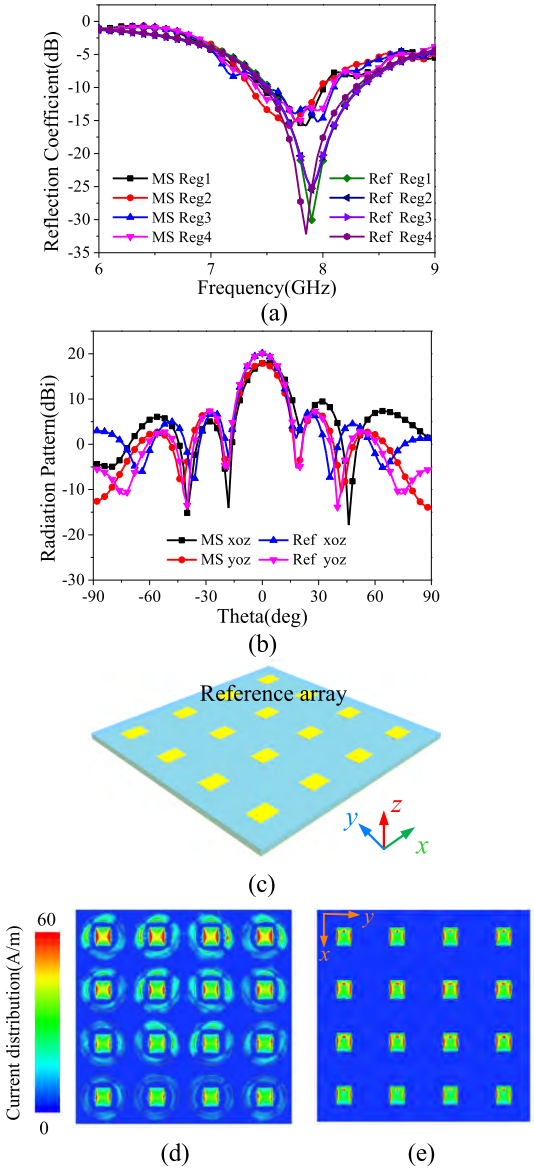

FIGURE 7. Radiation properties comparison between AEMS array and reference array. (a) Reflection coefficients. (b) 2D radiation patterns at 7.7GHz and 7.8GHz. (c) Geometry of reference array. (d) Current distributions on AEMS array at 7.7GHz. (e) Current distributions on reference array at 7.8GHz.

unit cell, PCS part rotation unit cell and a single radiation patch unit cell is analyzed, as shown in Fig. 5. Reflection coefficients of three units are in a basic coincidence.

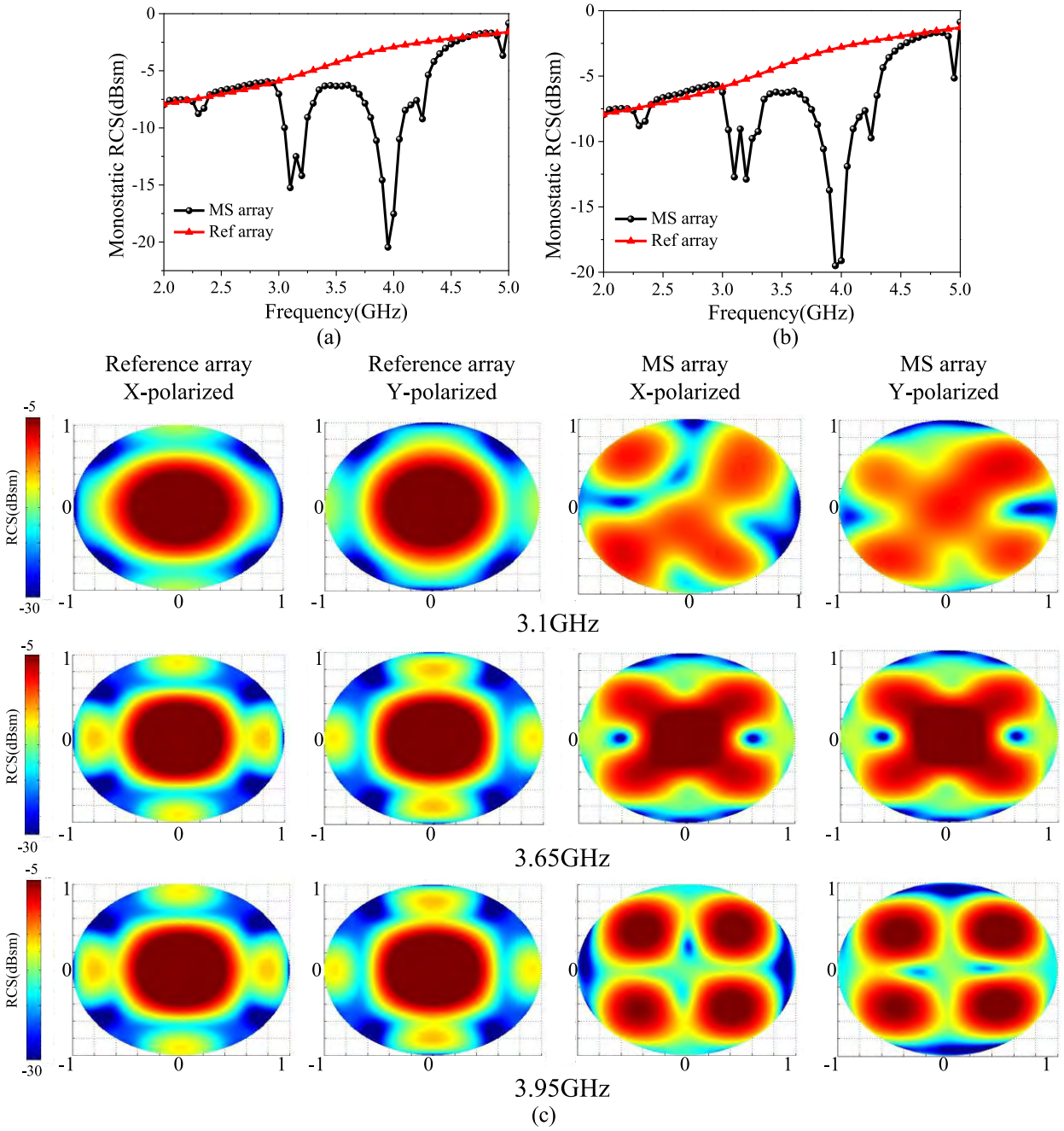

FIGURE 8. Scattering properties comparison between MS array and reference array. (a) Monostatic RCS under x-polarized incidence. (b) Monostatic RCS under y-polarized incidence. (c) 3D scattering fields of MS array and reference array at 3.1GHz, 3.65GHz and 3.95GHz.

The resonant frequency for the single patch unit is 7.8GHz. And for original unit and PCS rotation unit, the resonant frequency points are all 7.78GHz. Antenna gains in normal direction are also simulated, which are conforming to reflection coefficients. From the above analysis, it can be concluded good impedance matching are achieved. Fig. 5(b) shows 2D radiation patterns of three units at their resonant frequency points in xoz and yoz planes. For all of the three units, the beam widths in yoz plane are slightly wider than the beam widths in xoz plane which depends on the shape of the square patch and the position of feeding structure. 3D radiation patterns are also simulated, as shown in Fig. 5(c)-(e), we can see that the peak radiations are achieved in the broadside direction and the three units all achieve good radiation properties.

III. RADIATION AND LOW SCATTERING PERFORMANCE OF SHARED APERTURE METASURFACE ARRAY

As analyzed above, the proposed MS unit cell possesses good radiation property and the ability to manipulate reflection phases. To achieve radiation and low scattering performances

simultaneously, the famous chessboard configuration of MS array is presented. Fig. 6 show the schematic geometry of the proposed MS array which consists of 4 × 4 unit cells. The whole array is divided into four regions. In region 2 and 4, PCS parts of the units have been rotated 90° to have a phase difference with those in region 1 and 3. For the proposed MS array, reflection can be suppressed based on phase cancellation principle, concurrently, good radiation performance can be maintained due to the slight influence of PCS parts.

Radiation performances of MS array are firstly analyzed. The comparison between the proposed MS array and a reference array is presented. As shown in Fig. 7(c), the reference array contains 4 × 4 square patches without PCS parts. Fig. 7(a) shows reflection coefficients of the proposed two arrays, a random unit is selected in each region. For MS array, four curves coincide well with each other, the resonant frequency point is 7.7GHz. For the reference array, reflection coefficients values are lower and the resonant frequency point is about 7.8GHz. The comparison of 2D radiation patterns at resonant frequencies is depicted in Fig. 7(b). The main-beam patterns are all along normal direction. The peak gain of MS array is 18.1dBi while the reference array attains 20.1dBi. Side lobe levels of MS arrays are relatively low although they are slightly higher than those of reference array. Current distributions of two arrays are also investigated, as shown in Fig. 7(d) and 7(e). For the proposed two arrays, intense currents are all observed on square patches at 7.7GHz and 7.8GHz. However, slight currents are produced on PCS parts for MS array. Coupling effect occurs between radiation patches and PCS parts.

The phenomenon also explains the reason that little differences between MS and reference array in reflection coefficients and radiation patterns. To sum up, the proposed SA MS array performances good radiation performance.

Scattering performances of two arrays are also analyzed. Figs. 8(a) and 8(b) show the comparison of monstatic radar cross section (RCS) properties. It can be seen the RCS of AEMS array has a remarkable reduction from 2.9GHz to 4.2GHz under x-polarized incident waves. The reduction peak values attain 10.1dB and 17.2dB at 3.1GHz and 3.95GHz respectively. The results under y-polarized incidences are similar with those under x-polarized incidences', the RCS reduction band is from 3.0GHz to 4.3GHz with peak values of 7.2dB and 16.8dB. The reason is that MS unit PCR value at these two points are relatively high, most reflected waves are transformed and cancelled. To further reveal the reason of low backward scattering properties, scattering fields of two arrays at 3.1GHz, 3.65GHz and 3.95GHz are simulated respectively in uv-plane ($u = \sin\theta\cdot\cos\varphi$, $v = \sin\theta\cdot\sin\varphi$), as shown in Fig. 8(c). For the reference array, the main reflected lobes are all in the normal direction with relatively high values. However, for the AEMS array, the scattering fields are different. At 3.95GHz, the main reflected lobes are dispersed to four quadrants, $\varphi = 45°$, 135°, 225° and 315°. The phenomenon indicates that the reflection reduction is mainly achieved based on phase cancellation. At 3.1GHz, strong scattering fields are in diagonal distribution, and the reflected lobes in normal direction are reduced effectively. At 3.65GHz, the low backward scattering property is not obvious. As can be seen in the fields, only a small part of reflected energy has been dispersed to four quarters, and the main lobe levels are relatively high. The reason is that the unit PCR at this point is relatively low. Owing to the symmetrical structure of AEMS unit cell, the scattering fields under x-polarized and y-polarized incidences are basically consistent with each other.

From the above analysis, it can be concluded that low backward scattering performances of AEMS array are achieved.

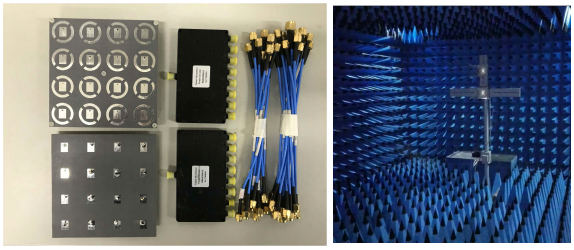

FIGURE 9. Prototypes of proposed MS and reference array. (a) Fabricated sample. (b) Test environment.

IV. SAMPLE FABRICATION AND EXPERIMENTS

To validate the performances mentioned above, we fabricated both MS array and reference array, as shown in Fig. 9(a). Two power dividers are exploited to equally distribute the input power. The vector network analyzer Agilent N5230C has been utilized to obtain the experimental data. Fig. 10(a) gives the measured reflection coefficients of the proposed two arrays. Similar with the simulated situation, four random units in each region are selected. The resonant frequencies of two arrays are almost close to 7.9GHz and 7.95GHz respectively. The measured results agree well with simulations, indicating that good impedance matching of MS array is observed. The comparison of normalized gain between two arrays is presented in Fig. 10(b). To eliminate noise interference, the testing results are measured in the anechoic chamber. It can be seen that main-beam patterns of two arrays are all along normal direction. For MS array, the side lobes are slightly higher than those of reference array. The agreement can be found between measured and simulated results.

Scattering performances of MS array for normal incident waves are also measured. Reflection reduction properties compared to reference array are depicted in Fig. 11. For x-polarized incident waves, the reflection reduction band is from 2.8GHz to 4.4GHz with peak value of 20dB. And for y-polarized incidences, obvious reduction is from 3.0GHz to 4.5GHz. The peak reduction value attains 19.5dB at 4.0GHz around. Measured results indicate that low backward scattering performances are achieved. However, compared

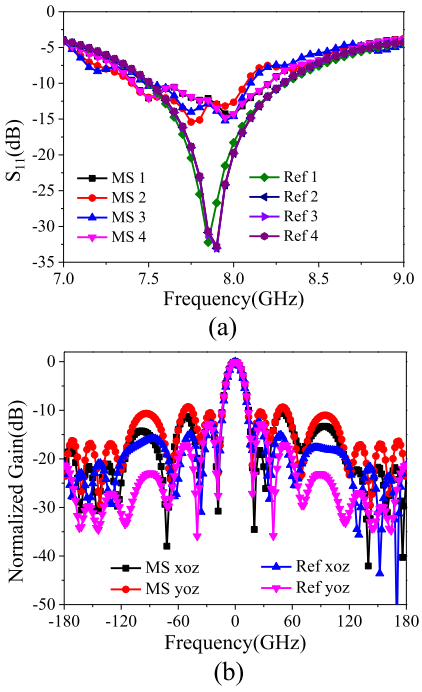

FIGURE 10. Measured radiation properties. (a) Reflection coefficients. (b) Radiation patterns at 7.9GHz and 7.95GHz.

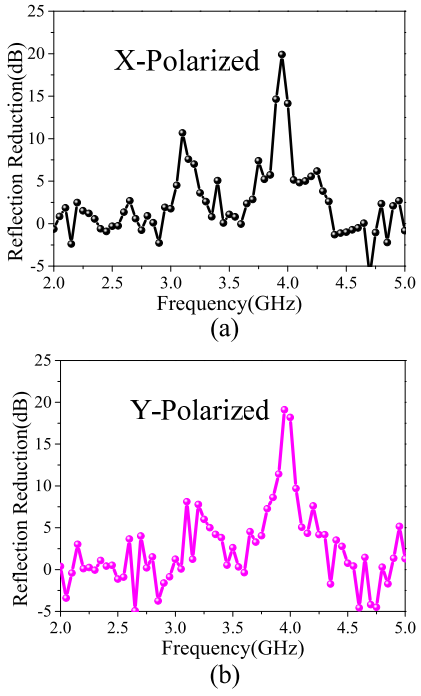

FIGURE 11. Measured reflection reduction. (a) Under x-polarized incidences. (b) Under y-polarized incidences.

with simulations, the measured results have some enhanced RCS points, especially in upper and lower bands of the chart and 3.5GHz around. The error is caused by the measurement noises and fabrication tolerance. In our future work, we will try to overcome these problems.

V. CONCLUSION

In conclusion, we proposed a novel method to design MS in this paper. Inspired by shared aperture technology, the MS possesses multiple functions, including radiation and low backward scattering performances. The MS unit consists of PCS part and radiation part, which are integrated together and can realize different functions. Radiation performance is achieved through adding feeding structure to each MS unit. Currently, two different MS units are arranged in chessboard array to realize low backward scattering performance. Both simulated and measured results show that good impedance matching and radiation performance are achieved. Moreover, the proposed MS possess low backward scattering properties compared with a reference array. It is worth noting that more various functions can be achieved through changing the arrangement of MS units, such as polarization conversion, anomalous reflection and diffusion. To sum up, this work provides an effective method to design multifunction MS and will lead to many exciting applications in different frequency domains.

ACKNOWLEDGMENT

(Chen Zhang and Xiangyu Cao contribute equally to this work.)

REFERENCES

[1] T. Frenzel, M. Kadic, and M. Wegener, "Three-dimensional mechanical metamaterials with a twist," *Science*, vol. 358, no. 6366, pp. 1072–1074, Nov. 2017.

[2] M. Choi *et al.*, "A terahertz metamaterial with unnaturally high refractive index," *Nature*, vol. 470, pp. 369–373, Feb. 2011.

[3] S.-J. Li *et al.*, "Ultra-wideband and polarization-insensitive perfect absorber using multilayer metamaterials, lumped resistors, and strong coupling effects," *Nano. Res. Lett.*, vol. 13, no. 1, p. 386, Dec. 2018.

[4] J. B. Pendry, D. Schurig, and D. R. Smith, "Controlling electromagnetic fields," *Science*, vol. 312, no. 5781, pp. 1780–1782, Jun. 2006.

[5] D. R. Smith, J. B. Pendry, and M. C. K. Wiltshire, "Metamaterials and negative refractive index," *Science*, vol. 305, no. 5685, pp. 788–792, Aug. 2004.

[6] X. Ni, K. N. Emani, A. V. Kildishev, A. Boltasseva, and V. M. Shalaev, "Broadband light bending with plasmonic nanoantennas," *Science*, vol. 335, no. 6067, p. 427, Jan. 2012.

[7] M.-X. Ren, W. Wu, W. Cai, B. Pi, X.-Z. Zhang, and J. J. Xu, "Reconfigurable metasurfaces that enable light polarization control by light," *Light Sci. Appl.*, vol. 6, no. 6, Jun. 2017, Art. no. e17085.

[8] C. Pelzman and S. Y. Cho, "Polarization-selective optical transmission through a plasmonic metasurface," *Appl. Phys. Lett.*, vol. 106, Jun. 2015, Art. no. 251101.

[9] F. Samadi, M. Akbari, M. R. Chaharmir, and A. Sebak, "Scatterer surface design for wave scattering application," *IEEE Trans. Antenna Propag.*, vol. 67, no. 2, pp. 1202–1211, Feb. 2018.

[10] Q. Ma, C. B. Shi, G. D. Bai, T. Y. Chen, A. Noor, and T. J. Cui, "Beam-editing coding metasurfaces based on polarization bit and orbital-angular-momentum-mode bit," *Adv. Opt. Mater.*, vol. 5, no. 23, Dec. 2017, Art. no. 1700548.

[11] L. Allen, M. W. Beijersbergen, R. J. C. Spreeuw, and J. P. Woerdman, "Orbital angular momentum of light and the transformation of laguerre-Gaussian laser modes," *Phys. Rev. A, Gen. Phys.*, vol. 45, no. 11, pp. 8185–8189, Jun. 1992.

[12] K. Zhang *et al.*, "Phase-engineered metalenses to generate converging and non-diffractive vortex beam carrying orbital angular momentum in microwave region," *Opt. Express*, vol. 26, no. 2, pp. 1351–1360, Jan. 2018.

[13] R. Singh, E. Plum, W, Zhang, and N. I. Zheludev, "Highly tunable optical activity in planar achiral terahertz metamaterials," *Opt. Express*, vol. 18, no. 13, pp. 13425–13430, Jun. 2010.
[14] X. Wen and J. Zheng, "Broadband THz reflective polarization rotator by multiple plasmon resonances," *Opt. Express*, vol. 22, no. 23, pp. 28292–28300, Nov. 2014.
[15] S. Sun, Q. He, S. Xiao, Q. Xu, X. Li, and L. Zhou, "Gradient-index metasurfaces as a bridge linking propagating waves and surface waves," *Nature Mater.*, vol. 11, no. 5, pp. 426–431, May 2012.
[16] W. Sun, Q. He, S. Sun, and L. Zhou, "High-efficiency surface plasmon meta-couplers: Concept and microwave-regime realizations," *Light Sci. Appl.*, vol. 5, no. 1, Jan. 2016., Art. no. e16003.
[17] A. Pors, M. G. Nielsen, T. Bernardin, J. C. Weeber, and S. I. Bozhevolnyi, "Efficient unidirectional polarization-controlled excitation of surface plasmon polaritons," *Light Sci. Appl.*, vol. 3, no. 8, p. e197, Aug. 2014.
[18] Y. J. Zheng *et al.*, "Ultra-wideband polarization conversion metasurface and its application cases for antenna radiation enhancement and scattering suppression," *Sci. Rep.*, vol. 7, Nov. 2017, Art. no. 16137.
[19] C. Zhang, J. Gao, X. Y. Cao, L. M. Xu, and J. F. Han, "Low scattering microstrip antenna array using coding artificial magnetic conductor ground," *IEEE Antennas Wireless Propag. Lett.*, vol. 17, no. 5, pp. 869–872, May 2018.
[20] B. Y. Sima, K. Chen, X. Y. Luo, J. M. Zhao, and Y. J. Feng, "Combining frequency-selective scattering and specular reflection through phase-dispersion tailoring of a metasurface," *Phy. Rev. Appl.*, vol. 10, Dec. 2018, Art. no. 064043.
[21] R. B. Hwang and Y.-L. Tsai, "Reflection characteristics of a composite planar AMC surface," *AIP Adv.*, vol. 2, Mar. 2012, Art. no. 012128.
[22] N. I. Landy, S. Sajuyigbe, J. J. Mock, D. R. Smith, and W. J. Padilla, "Perfect metamaterial absorber," *Phys. Rev. Lett.*, vol. 100, no. 20, May 2008, Art. no. 207402.
[23] S.-J. Li *et al.*, "Hybrid metamaterial device with wideband absorption and multiband transmission based on spoof surface plasmon polaritons and perfect absorber," *Appl. Phys. Lett.*, vol. 106, May 2015, Art. no. 181103.
[24] D. Shrekenhamer, W.-C. Chen, and W. J. Padilla, "Liquid crystal tunable metamaterial absorber," *Phys. Rev. Lett.*, vol. 110, no. 17, Apr. 2013, Art. no. 177403.
[25] Y. Zhao *et al.*, "Broadband diffusion metasurface based on a single anisotropic element and optimized by the simulated annealing algorithm," *Sci. Rep.*, vol. 6, Apr. 2016, Art. no. 23896.
[26] Z. C. Li, W. W. Liu, H. Cheng, J. Y. Liu, S. Q. Chen, and J. G. Tian, "Simultaneous generation of high-efficiency broadband asymmetric anomalous refraction and reflection waves with few-layer anisotropic metasurface," *Sci. Rep.*, vol. 6, Oct. 2016, Art. no. 35485.
[27] Y. Zhao, X. Y. Cao, J. Gao, and W.-Q. Li, "Broadband RCS reduction and high gain waveguide slot antenna with orthogonal array of polarisation-dependent AMC," *Electron. Lett.*, vol. 49, no. 21, pp. 1312–1313, Oct. 2013.
[28] T. J. Cui, M. Q. Qi, X. Wan, J. Zhao, and Q. Cheng, "Coding metamaterials, digital metamaterials and programmable metamaterials," *Light Sci. Appl.*, vol. 3, no. 10, p. e218, Oct. 2014.
[29] C. Huang, C. Zhang, J. Yang, B. Sun, B. Zhao, and X. Luo, "Reconfigurable metasurface for multifunctional control of electromagnetic waves," *Adv. Mater.*, vol. 5, no. 22, Nov. 2017, Art. no. 1700482.
[30] Y. Zheng, J. Gao, L. Xu, X. Cao, and T. Liu, "Ultrawideband and polarization-independent radar-cross-sectional reduction with composite artificial magnetic conductor surface," *IEEE Antennas Wirel. Propag. Lett.*, vol. 16, pp. 1651–1654, 2017.
[31] Y. Liu, Y. W. Hao, K. Li, and S. X. Gong, "Radar cross section reduction of a microstrip antenna based on polarization conversion metamaterial," *IEEE Antennas Wirel. Propag. Lett.*, vol. 15, pp. 80–83, 2015.
[32] H. H. Yang *et al.*, "A programmable metasurface with dynamic polarization, scattering and focusing control," *Sci. Rep.*, vol. 6, Oct. 2016, Art. no. 35692.
[33] S.-J. Li, J. Gao, X.-Y. Cao, Y. Zhao, Z. Zhang, and H.-X. Liu, "Loading metamaterial perfect absorber method for in-band radar cross section reduction based on the surface current distribution of array antennas," *IET Microw., Antennas Propag.*, vol. 9, no. 5, pp. 399–406, Apr. 2015.
[34] L. Zhang *et al.*, "Realization of low scattering for a high-gain fabry–perot antenna using coding metasurface," *IEEE Trans. Antenna Propag.*, vol. 65, no. 7, pp. 3374–3383, Jul. 2017.
[35] Y. Zhao, X. Cao, J. Gao, L. Xu, X. Liu, and L. L. Cong, "Broadband low-RCS circularly polarized array using metasurface-based element," *IEEE Antennas Wirel. Propag. Lett.*, vol. 16, pp. 1836–1839, 2017.
[36] K. Kandasamy, B. Majumder, J. Mukherjee, and K. P. Ray, "Low-RCS and polarization-reconfigurable antenna using cross-slot-based metasurface," *IEEE Antennas Wirel. Propag. Lett.*, vol. 14, pp. 1638–1641, 2015.
[37] Y. Liu, K. Li, Y. T. Jia, Y. W. Jia, S. X. Gong, and Y. J. Guo, "Wideband RCS reduction of a slot array antenna using polarization conversion metasurfaces," *IEEE Trans. Antenna Propag.*, vol. 64, no. 1, pp. 326–331, Jan. 2016.
[38] J.-D. Zhang, W. Wu, and D.-G. Fang, "Dual-band and dual-circularly polarized shared-aperture array antennas with single-layer substrate," *IEEE Trans. Antenna Propag.*, vol. 64, no. 1, pp. 109–116, Jan. 2016.
[39] M. Long, W. Jiang, and S. Gong, "Wideband RCS reduction using polarization conversion metasurface and partially reflecting surface," *IEEE Antennas Wireless Propag. Lett.*, vol. 16, pp. 2534–2537, 2017.

CHEN ZHANG was born in China, in 1992. He received the B.S. and M.S. degrees from the Information and Navigation Institute, Air Force Engineering University of CPLA, China, in 2014 and 2016, respectively, where he is currently pursuing the Ph.D. degree in electromagnetic field and microwave technology. He has authored or coauthored more than ten technical journal articles and conference papers. His research interest includes multifunctional metasurface and their antenna applications.

XIANGYU CAO (SM'08) received the B.S. and M.S. degrees from the Air Force Missile Institute (AFMI), Xi'an, China, in 1986 and 1989, respectively, and the Ph.D. degree in Missile Institute, Air Force Engineering University (AFEU), in 1999.

In 1989,and became an Associate Professor, in 1996. From 1999 to 2002, she was engaged with a Postdoctoral Research, Xidian University, China. She was a Senior Research Associate with the Department of Electronic Engineering, City University of Hong Kong, from 2002 to 2003. She is currently a Professor with AFEU. She has authored or coauthored more than 120 technical journal articles and conference papers. Her research interests include computational electromagnetic, smart antennas, electromagnetic metamaterial, and their antenna applications.

JUN GAO received the B.S. and M.S. degrees from the Air Force Missile Institute (AFMI), Xi'an, China, in 1984 and 1987, respectively. In 1987, he joined AFMI as an Assistant Teacher and became an Associate Professor, in 2000. He is currently a Professor with Air Force Engineering University (AFEU). His research interests include smart antennas, electromagnetic metamaterial, and their antenna applications.

SI-JIA LI received the B.Eng. degree in electronics and information engineering from Guangxi University, Nanning, China, in 2009, and the M.Eng. degree in information and telecommunication engineering from Air Force Engineering University, Xi'an China, in 2011, where he is currently pursuing the Ph.D. degree in electromagnetic field and microwave technology with the Information and Navigation Institute. He has authored or coauthored more than 40 scientific papers in major journals and international conferences. His research interest includes the broadband perfect metamaterial absorber and its application for RCS reduction of antennas.

HUANHUAN YANG (S'15) received the B.S., M.S., and Ph.D. degrees from Air Force Engineering University (AFEU), Xi'an, China, in 2010, 2012, and 2016, respectively. He was a Joint-Supervision Ph.D. Student with AFEU and Tsinghua University. He is currently a Lecturer with AFEU. His research interests include reconfigurable antenna, reflectarray, metasurface, and RCS reduction technique.

TONG LI received the B.S. and Ph.D. degrees in electronic and information engineering from Xidian University, Xi'an, China, in 2010 and 2015, respectively. She is currently a Lecturer with Air Force Engineering University. Her current research interests include ultrawideband communication devices, reconfigurable antennas, and metasurface.

DI ZHANG received the B.S. and M.S. degrees from Air Force Engineering University (AFEU), Xi'an, China, in 2013 and 2015, respectively, where he is currently pursuing the Ph.D. degree. His current research interests include RF OAM antennas, reflectarray antennas, and metasurface.